

# Air Filter Performance Under Variable Air Volume Conditions

**Richard D. Rivers**  
Fellow/Life Member ASHRAE

**David J. Murphy, Jr.**  
Member ASHRAE

## ABSTRACT

*Samples of 31 different air filters, representative of the designs and efficiency range of those used in general ventilation, were tested at constant airflow. The complete array of ASHRAE Standard 52.1 tests was run on these filters, plus particle-size efficiency tests and tests measuring the reentrainment of dust from the filters when subjected to ultra-clean air flow. Additional samples of the same filters were then subjected to the same test array, except that VAV flow was simulated. No significant difference was noted between the results using constant flow and VAV flow; low efficiency filters did, however, show substantial reentrainment for both cases. Additional studies of the filter media resistance showed that media resistance as a function of media airflow velocity can be predicted from media geometry more accurately than by existing theories if media compression under airflow is taken into account. Expressions for overall filter resistance as a function of filter flow and means for obtaining their coefficients are given.*

## INTRODUCTION

The overall goal of this study was to develop a means to predict air filter resistance and particle-size efficiency for air filters in HVAC systems operating in the variable air volume (VAV) mode. It is well known that the airflow resistance of filters is dependent on air velocity. In addition, the dust-capture efficiency of filters might be lower (or higher) when filters operate above or below the velocity recommended by their manufacturers for constant-flow systems.

There has also been concern that the intermittent rise and fall of air velocity through filter media under VAV operation might dislodge captured dust or even fracture media fibers enough to affect air quality significantly. The established

ASHRAE 52.1 Air Filter Test Standard (ASHRAE 1992) does not attempt to simulate variable air flow performance.

Past experience had shown that coarse-fiber, low-efficiency filters do retain captured dust rather poorly, while fine-fiber, high-efficiency filters do not show this effect significantly. It thus seemed appropriate to test a wide range of filter types, including designs with flexible gross structures as well as those that held their media in relatively rigid structures. A variety of filter media fibers and ASHRAE dust-spot efficiencies were also included in the samples studied. A two-stage ionizer/plate type electrostatic air cleaner was also included in the study to see if it, too, suffered efficiency degradation under VAV conditions.

Table 1 lists the characteristics of the 31 filter types tested, all of which are commercially available. This list includes most filter types currently used in general ventilation service. The cross sections of the filter configurations are shown schematically in Figure 1. The column "Media Code" in Table 1 identifies the 15 media types used in the 30 fibrous-media filters. These media are described in Table 2. Media samples were obtained from the manufacturers or, if that was not possible, by disassembly of filters.

## TESTING OF FULL-SIZE FILTERS

A sample of each of the 30 fibrous-media filters was subjected to the array of tests specified in ASHRAE Standard 52.1 at a constant air flow of 0.94 m<sup>3</sup>/s (2000 cfm). A second sample of each was then tested under VAV conditions, using a flow that varied in linear sawtooth pattern from 0.47 to 0.94 m<sup>3</sup>/s (1000 to 2000 cfm) in 60 seconds. This cycle was repeated 120 times during each VAV test. In addition, the particle-size efficiency of the filters was measured

---

**Richard D. Rivers** is president of EQS, Inc., Louisville, Ky. **David J. Murphy, Jr.**, was, at the time of his death, president of Air Filter Testing Laboratories, which he founded, in Crestwood, Ky.

**TABLE 1**  
**Summary Description of Filter Types**

Filter Code	Dust-Spot Efficiency Range, %	Generic Filter Type	Rigid/ Non-Rigid	Form	Depth (mm)	Media Code	Media Type	Media Area (m <sup>2</sup> )	Initial Resis. @ 0.94 m <sup>3</sup> /s Pa
1	90-95	Pleated, with separators	Rigid	C	267	38	Wet-laid glassfiber	10.03	140
2	90-95	Pleated, with ribbon spacers	Rigid	C	96	38	Wet-laid glassfiber	10.10	170
3	90-95	Cartridge, internal supports	Rigid	B	267	19	Air-laid glassfiber	5.20	215
4	90-95	Multipanel minipleat	Rigid	E	267	38	Wet-laid glassfiber	18.02	68
5	90-95	Nonsupported bag	Non	D	737	19	Air-laid glassfiber	7.71	130
6	90-95	Nonsupported bag	Non	D	625	35	Blown polypropylene	8.40	115
7	80-85	Pleated, with separators	Rigid	C	267	39	Wet-laid glassfiber	10.03	110
8	80-85	Pleated, with ribbon spacers	Rigid	C	96	39	Wet-laid glassfiber	10.10	155
9	80-85	Cartridge, internal supports	Rigid	B	267	20	Air-laid glassfiber	5.20	183
10	80-85	Multipanel minipleat	Rigid	E	267	39	Wet-laid glassfiber	18.02	78
11	80-85	Nonsupported bag	Non	D	737	20	Air-laid glassfiber	7.71	110
12	80-85	Nonsupported bag	Non	D	625	36	Blown polypropylene	8.40	118
13	60-65	Pleated, with separators	Rigid	C	267	40	Wet-laid glassfiber	10.03	78
14	60-65	Pleated, with ribbon spacers	Rigid	C	96	40	Wet-laid glassfiber	10.10	113
15	60-65	Cartridge, internal supports	Rigid	B	267	24	Air-laid glassfiber	5.20	110
16	60-65	Multipanel minipleat	Rigid	E	267	40	Wet-laid glassfiber	18.02	90
17	60-65	Nonsupported bag	Non	D	737	24	Air-laid glassfiber	7.71	63
18	60-65	Nonsupported bag	Non	D	625	37	Blown polypropylene	3.80	30
19	40-45	Cartridge, external supports	Rigid	B	280	16	Air-laid glassfiber	5.21	70
20	40-45	Cartridge, external supports	Rigid	B	280	31	Dual-density spun polyester	5.21	83
21	40-45	Cartridge, nonsupported	Non	D	330	16	Air-laid glassfiber	2.98	55
22	40-45	Cartridge, nonsupported	Non	D	330	22	Spun polyester	2.98	58
23	40-45	Cartridge, nonsupported	Non	D	356	31	Dual-density spun polyester	1.40	63
24	40-45	Cartridge, nonsupported with wire grid	Non	D	356	31	Dual-density spun polyester	1.40	60
25	20-25	Cartridge, nonsupported	Non	D	280	25	Spun polyester/cotton	2.23	68
26	20-30	Pleated panel	Rigid	B	48	25	Spun polyester/cotton	1.67	58
27	20-30	Pleated panel	Rigid	B	98	25	Spun polyester/cotton	2.41	63
28	20-30	Replacement pad	Rigid	A	48	31	Dual-density spun polyester	0.372	98
29	20-30	Ring panel	Rigid	A	25	33	Spun polyester	0.372	63
30	80-85	Ionizer/plate electronic	Rigid	F	128	NA	None	NA	28
31	<20	Industrial spun glass pad	Rigid	A	48	11	Spun fiberglass pad	0.372	33

The individual panels making up filters 4, 10, and 16 had depths of 25 mm.

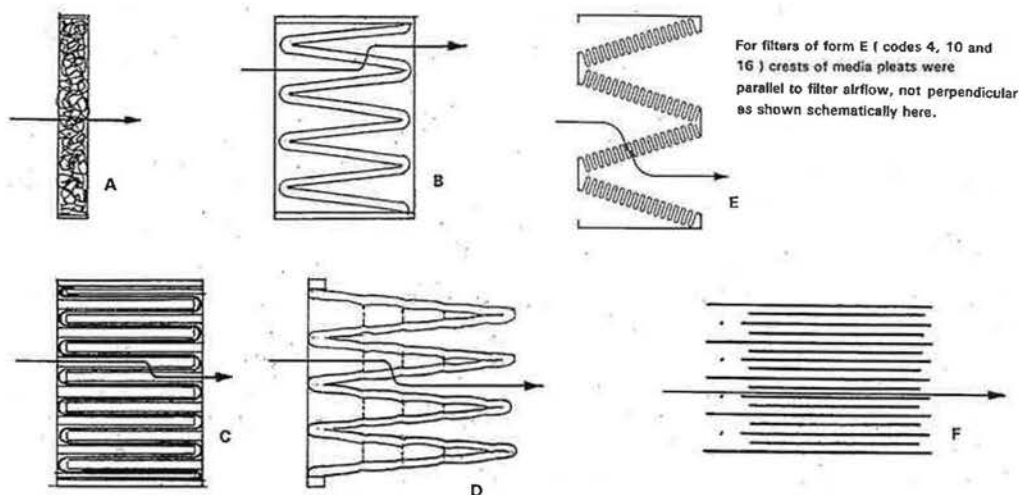


Figure 1 Basic forms of general ventilation filters.

TABLE 2  
Description of Filter Media Types

Media Code	Mfg. Stated Dust-Spot Efficiency Range, %	Type	Average Thickness Without Compression (mm)	Average Mass per Unit Area ( $\text{g}/\text{m}^2$ )	Average Binder Content, %	Fiber Diameter Range ( $\mu\text{m}$ )
11	<20	Spun glassfiber pad	60.2	216.0	34.9	9-36
16	40-45	Air-laid glassfiber, backed	7.5	95.5	24.4	4-7
19	90-95	Air-laid glassfiber, backed	7.5	71.9	29.6	1-3
20	80-85	Air-laid glassfiber, backed	9.6	67.7	14.6	1-3
22	40-45	Spun polyester, 6 mm thick	3.9	101.0	25.0	9-16
24	60-65	Air-laid glassfiber, backed	8.4	71.9	25.6	3-7
25	20-30	Spun polyester/cotton blend, 3 mm thick	3.9	86.3	20.0	7-16
31	40-45	Dual-density spun polyester, 25 mm thick	32.2	377.0	25.0	9-18
33	40-45	Spun polyester, 6 mm thick	23.2	160.0	25.0	24
35	90-95	Melt-blown polypropylene	2.6	95.6	0	18-24
36	80-85	Melt-blown polypropylene	2.5	89.5	0	20-24
37	60-65	Melt-blown polypropylene	8.2	103.0	0	9-18
38	90-95	Wet-laid glassfiber	0.54	75.6	3.1	2-5
39	80-85	Wet-laid glassfiber	0.53	75.2	5.1	3-6
40	60-65	Wet-laid glassfiber	0.71	73.5	6.7	4-7

All glassfibers except those in code 11 were melt-blown.

using a light-scattering particle counter, and the reentrainment of captured particles was measured by the same instrument. The sequence of tests was as follows:

1. Initial resistance traverse  $0-0.94 \text{ m}^3/\text{s}$  ( $0-2000 \text{ cfm}$ ). This test is a standard requirement of ASHRAE 52.1 and is useful in analyzing the sources of pressure loss (resistance) in the full-scale filter structure.

Thereafter, the following tests were run at a constant flow of  $0.94 \text{ m}^3/\text{s}$ :

2. Initial ASHRAE atmospheric dust-spot efficiency (DSE) using the "Constant-Flow" DSE method of ASHRAE 52.1, section 10.5.3. The dust source was ambient outdoor air in the rural Kentucky location of the test laboratory. At least five repeats of the test were performed and the median reported.

3. Particle reentrainment from the clean filter. This test was intended to detect whether the filter media itself contributed significant numbers of fibers or particles to the airstream. Ultra-clean (ULPA-filtered) air was passed through the filter. Particles downstream were detected using a white-light-scattering particle counter having 16 channels ranging from 0.3  $\mu\text{m}$  to 10  $\mu\text{m}$  particle diameter and one for particles greater than 10  $\mu\text{m}$ . The sample flow was 0.425  $\text{m}^3/\text{h}$  (0.25 cfm).
4. Initial particle-size efficiency, measured using the white-light-scattering particle counter described in test 3. The counter air sample was drawn from the upstream and downstream filter airflow alternately. The particle source was ambient atmospheric dust, without dilution.
5. ASHRAE dust holding capacity to a final resistance of 250 Pa (1.0 in WG). This is the test described in ASHRAE Standard 52.1, section 12.1.1, using ASHRAE standard test dust. This is both a standard performance index indicating the relative life of the filter in service and a means of validating any computer simulation of resistance-versus-dust load. The resistance of the filter at intermediate dust feed increments before the final increment was recorded in the course of the test.
6. ASHRAE initial and average arrestance over the period of dust feed. This is the test described in section 11 of ASHRAE Standard 52.1. The data obtained could be used to validate any computer simulation of dust collection in the filter, as well as for its usual characterization of the coarse-dust performance of the filter.
7. Final ASHRAE atmospheric dust-spot efficiency. This test repeated the procedure of test 1 on the fully loaded filter. It is a measure of the effect of dust load on DSE and will detect reentrainment of collected dust if it occurs.
8. Final particle-size efficiency. This was the same as test 4, but was performed after the filter was loaded with dust.
9. Particle reentrainment from the loaded filter. This test repeated test 3 on the dust-loaded filter; it shows whether the loaded filter and its collected dust contributes significant numbers of fibers or particles to the airstream.

After the above constant-flow tests, this test was run:

10. Final resistance traverse from 0 to 0.94  $\text{m}^3/\text{s}$  (0-2000 cfm). This test is useful in analyzing the sources of pressure loss (resistance) in the full-scale filter structure and in validating any computer simulation of dust collection in the filter.

The same sequence of tests was then performed on a second sample of each filter, but with 120 sawtooth flow cycles during tests 2, 3, 4, 7, and 8. The flow was held constant during the dust-loading procedures of tests 5 and 6 because the relatively coarse ASHRAE test dust would not be transported to the filters at near-zero airflows.

Final particle-size efficiencies (test 8) were not run on all filters because there was sufficient reentrainment to confuse the results using atmospheric dust, which cannot be distin-

guished from reentrained dust by the counter. Substantial reentrainment also produces agglomerates that may exceed the allowed count rate for the particle counter, block its inlet, or force cleaning of its optics. A negative efficiency from test 8 told that substantial reentrainment had occurred and test 9 should be skipped.

The ionizer/plate electrostatic air cleaner is cleaned when loaded, rather than discarded, as is the case with fibrous air filters. Loading this type of air cleaner with ASHRAE dust is not very meaningful. For comparison, and for possible use in efficiency simulation, we ran seven loading cycles on the filter tested, terminating each cycle when the filter DSE had dropped to nearly zero. This efficiency drop was probably the result of corona suppression in the ionizer or reduced voltage from the increased current draw when the filter is loaded with the rather conductive ASHRAE test dust. The resistance and arrestance of the electrostatic air cleaner both rose during each cycle, while DSE fell steadily. (See Figure 7.)

## RESULTS OF FULL-SIZE FILTER TESTS

Part I of the Final Report for Project 675-RP (Murphy and Rivers 1997) contains all the data gathered in the above tests. Figures 2 through 6 plot results for four of the filters tested: Codes 4, 12, 26, and 30. These are representative of the fibrous-media filters tested.

The tests of media degradation and dust dislodgement showed that the changes in filter flow under VAV operation do not materially damage any of the filters tested. A few low-efficiency filters showed noticeably higher loss of collected dust under VAV operation than under fixed-flow operation. Such filters show rather high losses of collected dust in either operating mode, so much so that not all tests could be performed on them.

Raw data from the reentrainment tests 3 and 9 illustrating this behavior for filter codes 4, 12, 26, and 30 is given in Table 3. The information obtained by the procedure is limited by the very low counts—often zero—obtained for particle diameters above about 3  $\mu\text{m}$ . It would take much longer counting periods, or loading of filters with uniformly sized particles above 3  $\mu\text{m}$ , to obtain quantitative data for large diameter particle reentrainment. The provision of “particle-free” air for the test is also difficult, as is shown by the data for upstream particle counts. Ideally, these should all be zero.

The absence of significant VAV effects leads us to conclude that a performance algorithm for VAV operation can be put together by treating the year as a series of intervals of fixed-flow operation. For each interval, the flow rates and dust conditions inside and outside the space served by the filter would be required. A computer program to do this is feasible, but practicing engineers will need a lot of guidance in the parameters to be inserted in such a program. They will also have to supply the pattern of flow quantities to be expected for the VAV system.

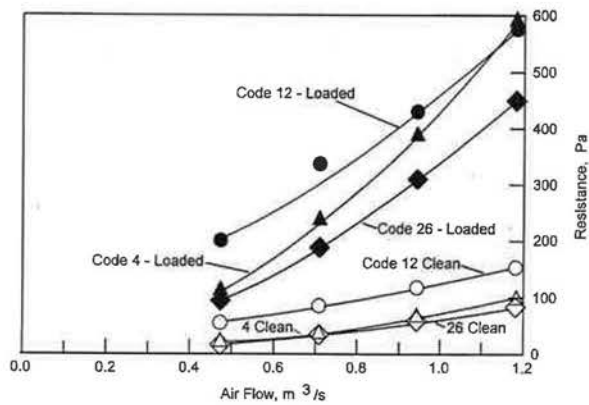


Figure 2 Resistance versus air flow.

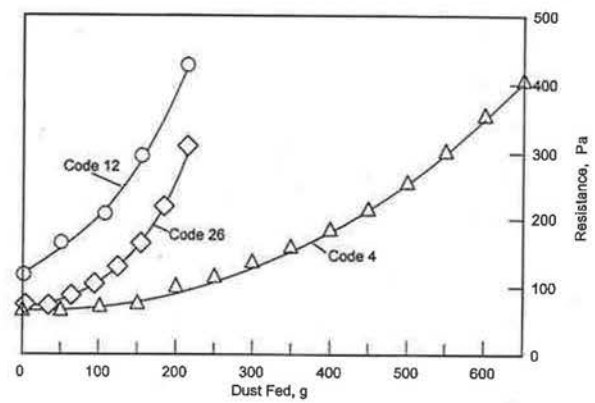


Figure 3 Resistance versus ASHRAE dust fed.

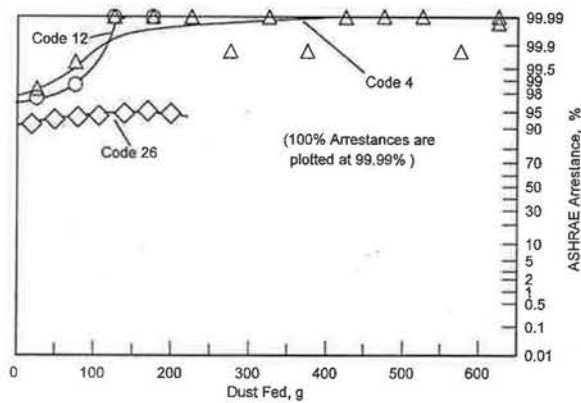


Figure 4 ASHRAE arrestance versus dust fed.

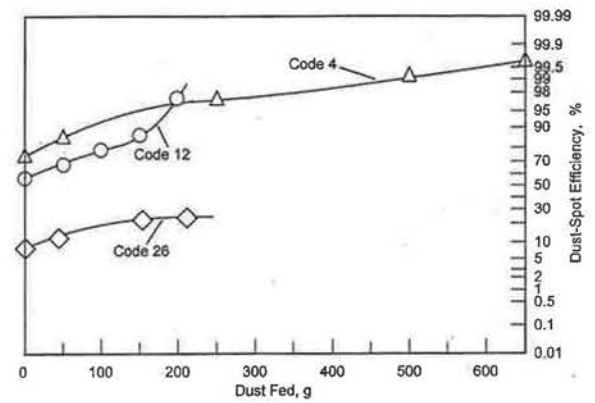


Figure 5 Dust-spot efficiency versus ASHRAE dust fed.

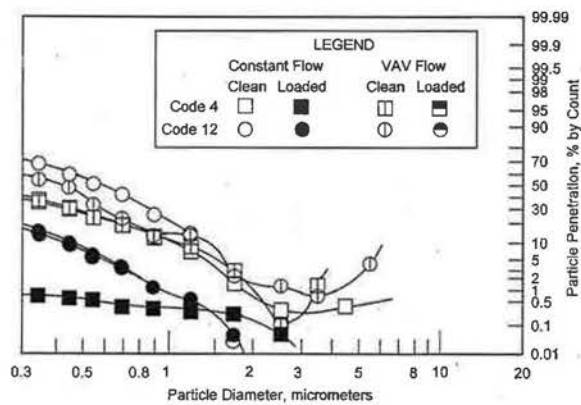


Figure 6a Particle penetration versus particle diameter—Code 4 and Code 12.

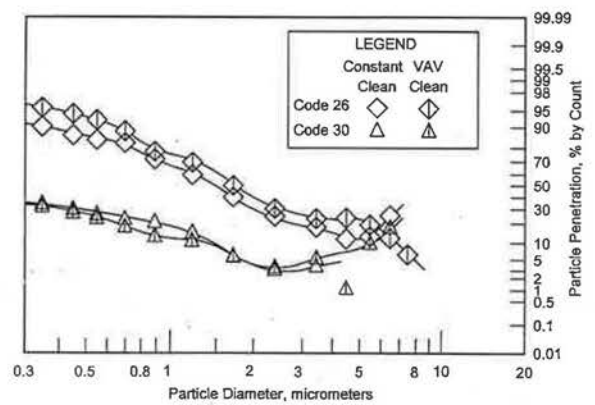
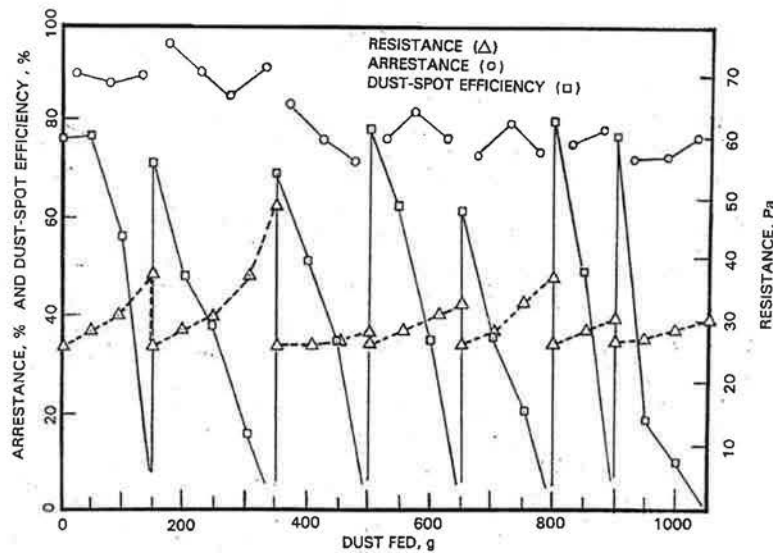


Figure 6b Particle penetration versus particle diameter—Code 26 and Code 30.





DUST FED WAS ASHRAE SYNTHETIC ARRESTANCE TEST DUST (72% STANDARD AIR CLEANER TEST DUST, FINE, 28% POWDERED CARBON, 5% COTTON LINTERS). DUST WAS FED IN 50 g INCREMENTS. FILTER WAS CLEANED WHEN DUST-SPOT EFFICIENCY APPROACHED ZERO.

AIR VELOCITY WAS 2.54 m/s (500 fpm), CORRESPONDING TO A FLOW OF 0.94 m<sup>3</sup>/s (2000 cfm).

**Figure 7** Two-stage ionizer-plate electrostatic precipitator (80%–85% dust-spot efficiency)—resistance, arrestance, and dust-spot efficiency versus dust load.

## DATA ANALYSIS

### Overall Filter Resistance

Several authors (Gunn and McDonough 1980; Raber 1982; Rivers 1990) have suggested Equation 1 as a first approximation to filter resistance as a function of velocity and dust load:

$$\Delta P_f = K_{ee} U_f^2 + K_m U_m \quad (1)$$

where

- $\Delta P_f$  = overall filter resistance
- $U_f$  = filter face velocity
- $U_m$  = average media velocity
- $K_{ee}$  = coefficient dependent on the gross geometry of the entrance and exit passages within the filter
- $K_m$  = coefficient dependent on media geometry, including the presence of captured dust

None of these references gives explicit means for calculating the coefficients  $K_{ee}$  and  $K_m$  or provide enough analysis to allow calculation of these resistances from filter geometry and air flow alone. In addition, they make the assumption that all the media is exposed and media velocity is uniform. In a well-designed filter, these assumptions are approximately true, but the influence of face and media velocity is overly simplified.

If the media velocity profile cannot be considered constant, the pattern of velocity and pressure would have to be

at least approximated and its influence on overall resistance determined. Solutions to the porous-walled duct problem for different three-dimensional geometries with reasonable wall pressure distributions would need to be undertaken. As Pui et al. (1991) showed, computational fluid dynamics can be used to model such situations for fairly simple geometries. In their case, the model was two-dimensional only.

We cannot imagine including the necessary software and instruction for its manipulation in a package intended for day-to-day design of filter systems, even if a reasonable model for gross flow into and out of each filter could be developed. We chose instead to work out a semi-empirical procedure with the following assumptions:

1. All media is exposed to airflow, and media velocity is uniform, hence:

$$U_m = Q_f / A_m \quad (2)$$

where

- $U_m$  = effective media velocity, m/s
- $Q_f$  = filter volumetric flow, m<sup>3</sup>/s
- $A_m$  = media area, m<sup>2</sup>

2. The resistance of the media at a given media velocity is the same in the filter as it is in a flat sheet with air flow perpendicular to the lay of the sheet.
3. Media resistance must include the effect of media compression at non-zero air flow, if such compression occurs at the media velocity calculated.

**TABLE 3a**  
**Particle Reentrainment from Clean and Dust-Loaded Filters:**  
**Counts with Ultra-Clean Air Flow (ULPA-Filtered)**

Code 4, 90–95% DSE 12-inch Multipanel Minipleat Filter, Wet-Laid Glassfiber Media																		
Air Flow	Dust Load, g	Location	Upstream and Downstream Particle Counts for Diameter Range (µm)															
			0.3–0.4	0.4–0.5	0.5–0.6	0.6–0.8	0.8–1.0	1.0–1.5	1.5–2.0	2–3	3–4	4–5	5–6	6–7	7–8	8–9	9–10	> 10
Const.	0	up	61	39	12	9	5	1	1	0	0	0	0	0	0	0	0	0
		down	16	5	2	2	0	0	0	0	0	0	0	0	0	0	0	0
VAV	0	up	32	20	11	8	2	4	0	0	0	0	0	0	0	0	0	0
		down	13	10	3	0	1	0	0	0	0	0	0	0	0	0	0	0
Const.	650	up	19	9	2	1	2	2	0	0	0	0	0	0	0	0	0	0
		down	9	9	1	6	2	8	7	4	0	0	0	0	0	0	0	0
VAV	650	up	11	5	1	1	0	0	1	0	0	0	0	0	0	0	0	0
		down	11	5	3	4	1	1	2	1	0	0	0	0	0	0	0	0
Code 12, 80–85% DSE Nonsupported Bag Filter, Blown Polypropylene Media																		
Air Flow	Dust Load, g	Location	Upstream and Downstream Particle Counts for Diameter Range (µm)															
			0.3–0.4	0.4–0.5	0.5–0.6	0.6–0.8	0.8–1.0	1.0–1.5	1.5–2.0	2–3	3–4	4–5	5–6	6–7	7–8	8–9	9–10	> 10
Const.	0	up	291	107	17	7	1	1	1	0	0	0	0	0	0	0	0	0
		down	114	41	5	1	0	2	0	0	0	0	0	0	0	0	0	0
VAV	0	up	305	116	17	11	2	3	2	0	0	0	0	0	0	0	0	0
		down	117	36	4	2	0	0	0	0	0	0	0	0	0	0	0	0
Const.	650	up	25	17	12	4	5	2	0	0	0	0	0	0	0	0	0	0
		down	2	1	1	0	0	0	0	0	0	0	0	0	0	0	0	0
VAV	650	up	33	25	15	7	2	0	1	0	0	0	0	0	0	0	0	0
		down	3	2	1	2	0	0	0	0	0	0	0	0	0	0	0	0

**TABLE 3b**  
**Particle Reentrainment from Clean and Dust-Loaded Filters:**  
**Counts with Ultra-Clean Air Flow (ULPA-Filtered)**

Code 26, 20-30% DSE Pleated 2-in Panel Filter, Spun Polyester-Cotton Blend Media:																		
Air Flow	Dust Load, g	Location	Upstream and Downstream Particle Counts for Diameter Range (µm)															
			0.3-0.4	0.4-0.5	0.5-0.6	0.6-0.8	0.8-1.0	1.0-1.5	1.5-2.0	2-3	3-4	4-5	5-6	6-7	7-8	8-9	9-10	> 10
Const.	0	up	74	68	19	11	0	3	3	0	0	0	0	0	0	0	0	0
		down	51	52	9	11	1	1	0	0	0	0	0	0	0	0	0	0
VAV	0	up	195	98	19	17	5	0	1	0	0	0	0	0	0	0	0	0
		down	246	155	31	38	8	3	2	0	0	0	0	0	0	0	0	0
Const.	210	up	1089	696	145	73	40	24	3	0	0	0	0	0	0	0	0	0
		down	1088	687	145	322	127	165	26	4	2	0	0	0	0	0	0	0
VAV	210	up	946	579	119	93	18	8	1	0	0	0	0	0	0	0	0	0
		down	1829	1459	496	1222	697	990	1056	210	17	5	1	0	0	0	0	0
Code 30, 80-85% DSE Two-Stage Ionizer-Plate Electrostatic Air Filter:																		
Air Flow	Dust Load, g	Location	Upstream and Downstream Particle Counts for Diameter Range (µm)															
			0.3-0.4	0.4-0.5	0.5-0.6	0.6-0.8	0.8-1.0	1.0-1.5	1.5-2.0	2-3	3-4	4-5	5-6	6-7	7-8	8-9	9-10	> 10
Const.	0	up	404	521	27	28	10	5	0	2	0	0	0	0	0	0	0	0
		down	476	475	17	25	12	4	4	1	1	0	0	0	0	0	0	0
VAV	0	up	1178	611	50	59	22	36	15	1	1	0	0	1	0	0	0	0
		down	1169	497	54	68	26	18	4	1	1	0	0	0	0	0	0	0

(No particle counts were made on the Code 30 electrostatic filter after dust was fed to it.)



4. Equation 1 is not correct; instead,

$$\Delta p_f = K_{ee} U_f^N + f(U_m, \mu, \alpha, \beta, x, R_f, Kn, M) \quad (3)$$

where

$R_f$  = fiber radius,  $\mu\text{m}$

$Kn$  = fiber Knudsen number =  $\lambda/R_f$  (4)

where

$\lambda$  = mean free path of the gas molecules, about 0.0663  $\mu\text{m}$  for standard air

$\alpha$  = volumetric fraction of solids in the media

$\beta$  = a factor specifying the nonuniformity of the media

$x$  = media thickness, mm

$\mu$  = gas viscosity,  $\text{Ns/m}^2$

$N, K_{ee}$  = experimentally determined constants

$M$  = dust load per unit area of media,  $\text{kg/m}^2$

The first step in this analysis was to determine the form of the function  $f(U_m, \mu, \alpha, \beta, x, R_f, Kn, M)$  in Equation 3 best applicable to all media tested in the clean condition. This was done on flat-sheet samples, as described under "Media Studies" below. Curve-fitting of resistance traverses on clean filters then gave both  $K_{ee}$  and  $N$ :

$$\begin{aligned} \ln[\Delta p_f - f(U_m, \mu, \alpha, \beta, x, R_f, Kn, M)] \\ = N \ln[U_f] + \ln[K_{ee}] \end{aligned} \quad (5)$$

## MEDIA STUDIES

The 15 fibrous media used in 30 of the 31 filters tested were also evaluated as flat-sheet samples. (Filter code 30 was an electrostatic air cleaner, which had no fibrous media). Media thickness and resistance were measured as a function of media velocity. A rough measure of media fiber diameter distributions was made using a visible-light microscope.

Below we discuss previous theories on which an expression for resistance could be based and the agreement between these theories and the data obtained in this study. One useful thing about the data collected here is that it covers the whole span of general-ventilation filter media. It appeared that most theoretical expressions for filter-media resistance had been verified with data obtained on a limited range of filter media. In addition, the effect of filter media compression from the airflow itself had been largely ignored by earlier investigators.

A procedure for including this effect was developed. It was then possible to select the theoretical expression for media resistance as a function of media geometry best fitting the entire range of media tested. Conversely, the mean fiber diameter of any fibrous media can be calculated using the relatively simple resistance and media compression measurements described. This calculated fiber diameter should remain constant for all air flows, if the theory accurately expresses the relation between media parameters and resistance. When fiber

diameter and media solids content are known, media efficiency as a function of particle diameter can be calculated from existing theory with satisfactory accuracy.

Media resistance theories are either purely empirical or based on some model defining the airflow field through the media. The flow field depends on the spacing, orientation, and diameter distribution of the media fibers and on gas properties. If the flowing gas is low enough in density, or the media fibers are so fine that their diameter approaches the mean-free-path of the gas molecules, the gas no longer behaves as a continuous fluid; "slip" takes place at the fiber surface. Preliminary fits to resistance data that ignored slip yielded fiber diameters that increased markedly as flow velocity increased. Clearly, slip must be taken into consideration for all but the coarsest fiber general ventilation filters. When this is done, several different flow-field expressions gave reasonable fits to the resistance data and reasonable predictions of mean fiber diameters.

Complete data for media characterization is given in Part I and Part II of the Final Report of Project RP-675 (Murphy and Rivers 1997). We summarize the results here.

## Measurement of Media Resistance

Flat-sheet resistance traverses were run in a 344 mm diameter test duct. Seven samples of each media were evaluated separately. The range of superficial media velocities chosen were the values to be expected when the media were operating in a full-scale filter. Samples of a given media code were reasonably uniform with respect to resistance.

Functions for media resistance versus average media approach velocity were obtained by least-squares polynomial fits to these data. None of the media showed a reasonable fit with a purely linear function; the function used for all was

$$\Delta p = a_r U_m + b_r U_m^2 \quad (6)$$

where  $\Delta p$  is media resistance, Pa, and  $U_m$  is superficial media velocity, m/s.

The coefficient  $a_r$  was always positive, as one would expect. Coefficient  $b_r$  was positive in nine cases, which one would expect for media that compress somewhat as air velocity and, hence, resistance increase. However, in six cases, coefficient  $b_r$  was clearly negative, as shown in Table 4. Our explanation for this is that where  $b_r$  is small relative to  $a_r$ , the media stretches slightly, actually decreasing superficial media velocity over the value obtained by dividing media sample flow by sample area. Since  $a_r$  and  $b_r$  are calculated for several values of  $U_m$  using Equation 2, if we use Equation 6 in further analysis of resistance, there would appear to be little harm in accepting negative as well as positive  $b_r$ . The three cases where  $b_r$  was negative—but still a substantial fraction of  $a_r$ —were all for thin, paperlike glassfiber media operating at low velocity. The effect of stretch on these media is quite small.

**TABLE 4**  
**Filter Media Resistance Coefficients**

Media Code	Media Type	Resistance Coefficients	
		$a_r$	$b_r$
11	Spun glassfiber pad	4.958	3.242
16	Air-laid glassfiber, backed	13.185	93.741
19	Air-laid glassfiber, backed	497.781	245.868
20	Air-laid glassfiber, backed	204.796	241.565
22	Spun polyester, 6 mm thick	8.218	-2.917
24	Air-laid glassfiber, backed	49.068	143.052
25	Spun polyester/cotton blend, 3 mm thick	34.556	-23.368
31	Dual-density spun polyester, 25 mm thick	16.787	6.468
33	Spun polyester, 13 mm thick	2.039	2.316
35	Melt-blown polypropylene	60.124	0.151
36	Melt-blown polypropylene	39.675	0.180
37	Melt-blown polypropylene	7.967	-0.005
38	Wet-laid glassfiber	892.935	-922.390
39	Wet-laid glassfiber	638.826	-243.008
40	Wet-laid glassfiber	227.339	-227.425

Resistance function is  $\Delta p_m = a_r U_m + b_r U_m^2$ , with  $\Delta p_m$  in Pa,  $U_m$  in m/s.

### Measurement of Media Compression

Media samples were stacked two to ten sheets high. An aluminum plate was placed on top of the stack, producing a pressure equivalent to 16 Pa on the stack. The stack height (minus plate thickness) was measured. Additional weights were then added to simulate the force exerted on the media by airflow resistance, up to a resistance of 250 Pa. It was apparent that all but one of the media types compressed significantly under pressures that might be seen in a clean or dust-loaded filter. A correction for media compression with resistance (whether due to velocity changes or dust accumulation or both) is therefore important to our filter performance model. The function used to fit the media compression data was

$$\ln(x) = a_c + (\Delta p)b_c + (\Delta p)^2 c_c \quad (7)$$

where

$x$  = media thickness, mm

$\Delta p$  = media resistance, Pa

The data fits showed that either or both of coefficients  $b_c$  and  $c_c$  could be zero, but not  $a_c$ . For rigid media, both  $b_c$  and  $c_c$  are zero.

Table 5 lists the values of  $a_c$ ,  $b_c$ , and  $c_c$  for the 15 media codes. Correlation coefficients for all these fits were in excess of 0.89.

### Measurement of Media Fractional Solids

A factor that appears constantly in expressions for filter media resistance and particle-capture efficiency is media fractional solids,  $\alpha$ :

$$\alpha = (10)M_m[(100 - P_b)/(\rho_f) + P_b/(\rho_b)]/X \quad (8)$$

where

$M_m$  = mass of media per unit area, kg/m<sup>2</sup>

$\rho_f$  = density of fiber, kg/m<sup>3</sup>

$\rho_b$  = density of binder, kg/m<sup>3</sup>

$P_b$  = percent (by mass) of binder in media

$X$  = the media thickness, m

The density of the fiber and media binders were taken from the literature (Table 6). Percent binder was obtained for glassfiber media by baking the media at high temperature to burn out the organic binder. For synthetic fiber media, we relied on information supplied by their manufacturers.

### DETERMINATION OF EFFECTIVE FIBER DIAMETER BY RESISTANCE MEASUREMENT

Flow in practical general-ventilation media is never turbulent, at least for any appreciable distance into the filter media. The highest Reynolds numbers observed are about 20. The starting point for the laminar flow of a viscous gas through a porous bed or mat is the equation of Darcy (1856),<sup>1</sup>

$$\Delta p_m = k_d U_m \mu X \quad (9)$$

where

$\Delta p_m$  = media resistance, Pa;

$k_d$  = a dimensionless constant.

Dimensional analysis (e.g., Davies 1973) allows one to express the Darcy constant  $k_d$  in terms of the fiber radius  $R_f$  and a function of the fractional solids in the filter,  $\alpha$ :

$$\Delta p_m = (U_m \mu X)[f(\alpha)]/R_f^2 \quad (10)$$

Davies developed an empirical expression for  $f(\alpha)$  by tests on filters having a fairly wide range of  $R_f$  and  $\alpha$ . Most of the studies of media resistance contain theoretical analyses that derive  $f(\alpha)$  using the Navier-Stokes equations for the gas flow through assumed models for the spacing and orientation

<sup>1</sup> One of the authors (RDR) had the pleasure of reading an original copy of this venerable treatise in the library of the city of Dijon, France, in 1996. Its title (translated) is "The Public Fountains of the City of Dijon." Thereafter, I walked across the central square of the city—Place Darcy—to the handsome Jardin Darcy, where the fountains that prompted Darcy's work have played gloriously for over 140 years. What other city in the world so honors a plumbing engineer?

**TABLE 5**  
**Filter Media Compression Coefficients**

Media Code	Media Type	Mass/Area (g/m <sup>2</sup> )	Binder Type	Binder (%)	Compression Coefficients		
					$a_c$	$b_c$	$c_c$
11	Spun glassfiber pad	216.4	1	34.9	4.098	-0.01476	2.829e-5
16	Air-laid glassfiber, backed	95.5	2	24.4	2.012	-0.00379	5.492e-6
19	Air-laid glassfiber, backed	71.9	2	29.6	2.047	-0.00615	1.522e-5
20	Air-laid glassfiber, backed	67.7	2	14.6	2.262	-0.00680	1.503e-5
22	Spun polyester, 6 mm thick	101.0	3	25.0	1.359	-0.00058	0
24	Air-laid glassfiber, backed	71.9	2	25.6	2.122	-0.00611	1.272e-5
25	Spun polyester/cotton blend, 3 mm thick	86.3	4	20.0	1.345	-0.00604	1.534e-5
31	Dual-density spun polyester, 25 mm thick	376.5	3	25.0	32.220	0	0
33	Spun polyester, 13 mm thick	160.4	3	25.0	3.143	-0.00878	2.217e-5
35	Melt-blown polypropylene	95.6	5	0	0.970	-0.00181	0
36	Melt-blown polypropylene	89.5	5	0	0.928	-0.00511	1.281e-5
37	Melt-blown polypropylene	102.8	5	0	2.109	-0.00180	0
38	Wet-laid glassfiber	75.6	1	3.1	-0.616	-0.00064	0
39	Wet-laid glassfiber	75.2	1	5.1	-0.641	-0.00077	0
40	Wet-laid glassfiber	73.6	1	6.7	-0.337	-0.00323	8.389e-6

Compression function is  $\ln(x) = a_c + (\Delta p_m) b_c + (\Delta p_m)^2 C_c$ , with  $x$  in mm,  $\Delta p_m$  in Pa.

of the filter fibers. Some have managed to develop reasonably rigorous expressions that include corrections for a distribution of fiber diameters, rather than the uniform fiber diameter implied by Equation 10. Some analyses include the effect of random variations in fractional solids and filter mat thickness, which mimics actual filter media more accurately. Ultimately, however, the random structure of most filter media cannot be modeled very well, and one or more empirical constants must be inserted to make measured resistances match theory. In our model, we assume that media behavior can be described well enough by using a single "effective" fiber diameter ( $R_f$ ), rather than attempting to determine the influence of fiber distribution.

If the flow regime is other than continuum flow, it is necessary to make corrections for the behavior of the gas at the fiber surface. These corrections depend on the Knudsen number of the fiber/gas combination, as described earlier. In this case, Equation 10 would be

$$\Delta p_m = (U_m \mu X) [f(\alpha, Kn)] / R_f^2 \quad (11)$$

Some studies (e.g., Wheat 1963) have expressed the effect of slip using Cunningham's factor (for the fiber),  $C_{gf}$ , instead of the Knudsen number,  $Kn$ :

$$\Delta p_m = (U_m \mu X) [f_2(\alpha, C_{gf})] / R_f^2 \quad (12)$$

The functions  $f(\alpha, Kn)$  or  $f_2(\alpha, C_{gf})$  are usually referred to as the "hydrodynamic function" for the media.

Equations 9 through 12 contain the variable  $\alpha$ , fractional solids. The actual value existing in the media at the flow velocity  $U$  must be inserted in the equation to determine  $\Delta p_m$ . However, as we have shown, most media compress when subjected to airflow drag; in these cases,  $\alpha$  is itself a function of  $\Delta p_m$ . This dependency has been blithely ignored by all but a few references that we found on fibrous media flow resistance and particle capture efficiency. Beavers et al. (1975) included the structural properties of the fibrous media in their resistance analysis to determine  $\alpha$  at each resistance. They had to assume a very simplified media structure to make this analysis. Chao and Chang (1982) included compression but substituted a pore-based efficiency calculation. Hollingsworth (1978), Magee et al. (1973), Ogorodnikov et al. (1976), Rüdinger and Wilhelm (1982), Tosun and Willis (1983), and Bergman et al. (1980) all mention that air filter media do compress but then develop expressions based on rigid media only.

Equations 11 and 12 can be rearranged to give  $R_f$  as a function of  $\Delta p_m$ :

$$R_f = \{ (U_m \mu X) [f(\alpha, Kn)] / \Delta p_m \}^{0.5} \quad (13)$$

$$R_f = \{ (U_m \mu X) [f_2(\alpha, C_{gf})] / \Delta p_m \}^{0.5} \quad (14)$$

**TABLE 6**  
**Fiber and Binder Densities**

Code	Material	Referenced Densities (g/cm <sup>3</sup> )	Chosen (g/cm <sup>3</sup> )
<b>Fibers:</b>			
1	cotton	1.52 (1) 1.54–1.59 (2)	1.55
2	glass insulation	2.5–2.58 (4) 2.47 (7)	2.54
3	polyester	1.32–1.40 (3) 1.31–1.43 (6)	1.36
4	polypropylene	0.90–0.92 (6)	0.92
5	50% polyester 50% cotton	average of codes 1 & 3	1.46
<b>Binders:</b>			
6	melamine-formaldehyde	1.47–1.52 (4) 1.40–1.55 (3)	1.45
7	phenol-furfural	1.32–1.42 (3)	1.35
8	phenol-formaldehyde	1.27 (3) 1.32–1.55 (5)	1.27
9	urea-formaldehyde	1.47–1.52 (5) 1.45–1.55 (3)	1.45
10	polyvinylacetate	1.15–1.45 (3)	1.30

**Refs.:** (1) Jonas et al. 1972; (2) Iinoya et al. 1970; (3) Dean 1985; (4) Christensen et al. 1993; (5) Weast and Astle 1979; (6) Machine Design 1985; (7) ASHRAE Handbook 1993

The most reliable expression for Cunningham's factor appears to be a function of Knudsen number alone, given by Allen and Raabe (1985):

$$C_{gf} = 1.142 + 0.558 \exp(-0.999/Kn) \quad (15)$$

For this reason, Equation 14 can always be implicitly expressed by Equation 13.

A computer program was written to calculate  $R_f$  from the factors on the right-hand side of Equation 13 using eight expressions for the fibrous media hydrodynamic function  $f(\alpha, Kn)$  from earlier studies. The aim was to determine which expression best predicted  $R_f$  for the 15 media in our study when media compression was included. Expressions that did not include the effect of slip flow were poor predictors. Expressions with slip-flow correction were then considered. The studies used were Natanson (1962), as modified by Pich (1966); Spielman and Goren (1968); Glushkov (1970); Chmielewski and Goren (1972); Kirsch et al. (1973); Ushak-

ova et al. (1973); Yeh and Liu (1974); and Monson (1986), as modified by Schaefer et al. (1986).

Two criteria were used to evaluate the hydrodynamic functions:

1. The ability of the function to yield fiber radii that most nearly approximated the values measured by microscopy for the whole range of samples studied.
2. Since the physical diameter of the fibers in a clean media remain constant for all media velocities, the  $(\alpha, Kn)$  function should produce the same  $R_f$  for all four velocities used in the tests of a given media. We used the percent standard deviation of the four values for each media as the index for this criterion; the lower the percent standard deviation, the better the function is.

It is difficult to select the best from the eight hydrodynamic functions tested on the basis of constancy of  $R_f$  calculated from Equation 13 at the four test velocities, but Natanson-Pich appears slightly better than the others. In addition, its predicted  $R_f$  fall within the range measured by microscope for media codes 11, 19, 24, 25, 38, 39, and 40. For codes 35, 36, and 39, the predicted  $R_f$  are slightly below the lower diameters observed under the microscope and for code 39, close to the upper diameter observed. For codes 16, 22, 31, 33, and 37, the predicted  $R_f$  are all higher than the upper microscopic value (by factors of 1.6, 2.0, 1.5, 1.5, and 2.0), but these are all closer than those predicted by the other seven hydrodynamic functions.

The Natanson-Pich function, dating from 1966, is explicit and easy to calculate, which is highly desirable. Its form is:

$$f(\alpha, Kn) = \frac{8\alpha(1 + 1.996Kn)}{1.5 - \ln(\alpha) + 2\alpha - 0.5\alpha^2 + 1.996Kn(-\ln(\alpha) + \alpha^2)} \quad (16)$$

## CALCULATION OF FILTER CONFIGURATION RESISTANCE

Once the effective fiber diameter for a filter's media is determined, one can determine the "configuration resistance" for the filter, the term  $K_{ee} U_f^N$  in Equation 3. This term is the pressure drop needed to get the air into and out of the filter, the difference between overall filter resistance and clean media resistance. Using the Natanson-Pich expression (Equation 16) for  $f(\alpha, Kn)$ , we have:

$$K_{ee} U_f^N = \Delta p_f - \left[ \frac{8\alpha(1 + 1.996Kn) U_m \mu X}{1.5 - \ln(\alpha) + 2\alpha - 0.5\alpha^2 + 1.996Kn(-\ln(\alpha) + \alpha^2) R_f^2} \right] \quad (17)$$



Taking the logarithm of both sides of Equation 17,

$$\ln(K_{ee}) + N \ln(U_f) = \ln \left\{ \Delta p_f - \left[ \frac{8\alpha(1 + 1 \cdot k)U_m \mu X}{1.5 - \ln(\alpha) + 2\alpha - 0.5\alpha^2 + 1.996Kn(-\ln(\alpha) + \alpha^2)R_f^2} \right] \right\} \quad (18)$$

A least-squares linear regression of the data using Equation 18 yields the best values for both  $K_{ee}$  and  $N$  for each filter. Values for  $N$  ranged from 1.15 to 3.74. A possible explanation for  $N$  exceeding 2 is that the filter pleats are collapsing against each other, reducing the flow area and increasing air velocity between pleats. Values of  $N$  below 2 could be caused by opening of pleats (or tubes, in the case of bag filters) as flow increases. Regardless of these effects, the procedure predicts overall filter resistance  $\Delta P_f$  quite well for the entire range of filter types and velocities. Codes 31 and 33 are flat sheets of media and have no configuration resistance; for them, there should be no  $K_{ee}U_f^N$  term, and, indeed, for them, calculated values of  $K_{ee}$  were small.

## CONCLUSIONS

As stated above, we observed no significant decrease in filter performance under VAV operating conditions, except for the very lowest efficiency filters. Theory predicts that efficiency varies with particle size and filter velocity for both fibrous filters and plate-type electronic air cleaners. This means that dust buildup in filter structures is dependent on the particle size distribution in the air approaching the filter, the filter velocity, and the dust previously collected.

The calculations of efficiency and resistance taking all these factors into consideration require considerable computer programming. An algorithm to accomplish this, based on established theories of inertial and diffusional particle capture and on the formation of "dendrites" by captured dust (Cai 1992), is outlined in the Final Report for Project RP-675 (Murphy and Rivers 1997). The algorithm would require validation by tests using well-defined aerosols. Such tests were beyond the scope of RP-675.

In addition the characteristics of aerosols met in various building situations would need to be established, and the engineer using the program would need to supply the pattern of airflow to the filtered space by season, time of day, and space occupancy. A program to calculate particulate air quality and its effect on filter performance envisaged here will need substantial work, but it appears feasible.

## REFERENCES

- Allen, M.D., and O.G. Raabe. 1985. Slip correction measurements of spherical solid aerosol particles in an improved Millikan apparatus. *Aerosol Sci. and Tech.* 4 (3): 269-286.
- ASHRAE. 1992. *ANSI/ASHRAE Standard 52.1-1992, Gravitric and dust spot procedures for testing air cleaning devices used in general ventilation for removing particulate matter*. Atlanta: American Society of Heating, Refrigerating and Air-Conditioning Engineers, Inc.
- ASHRAE. 1993. *1993 ASHRAE Handbook—Fundamentals*. Atlanta: American Society of Heating, Refrigerating and Air-Conditioning Engineers, Inc.
- Beavers, G.S., T.A. Wilson, and B.A. Masha. 1975. Flow through a deformable porous material. *Trans. ASME—Journal of Appl. Mech.*, pp. 598-602.
- Bergman, W., W.D. Kuhl, W.L. Russel, R.D. Taylor, H.E. Hebard, A.R. Biermann, N.J. Alvarez, D.G. Beason, and B.Y. Lum. 1980. Electrofibrous prefilters for use in nuclear ventilation systems. *Proc. 16th DOE Nuclear Air Cleaning Conf.*, pp. 807-837.
- Cai, J. 1992. Fibrous filters with non-ideal conditions. Dissertation, Royal Institute of Technology, Stockholm. (ISSN 0346-2668)
- Chao, C.C.M., and W.V. Chang. 1982. Pressure drop across compressible random-fiber porous medium: A unified filtration theory. *Proc. 3d World Filtration Cong.*, 2: 610-617.
- Chmielewski, R.D., and S.L. Goren. 1972. Aerosol filtration with slip flow. *Envir. Sci. & Technol.* 6 (13): 1101-1105.
- Christensen, V.R., W. Eastes, R.D. Hamilton, and A.W. Struss. 1993. Fiber diameter distributions in typical MMVF wool insulation products. *Am. Indus. Hyg. Assoc. J.* 54 (5): 232-238.
- Darcy. 1856. *The public fountains of the city of Dijon* (in Fr.). Dalmont, Paris.
- Davies, C.N. 1973. *Air filtration*, chapter 4. London: Academic Press.
- Dean, J.A., ed. 1985. *Lange's handbook of chemistry*, 13th ed. New York: McGraw-Hill.
- Glushkov, Y.M. 1970. Passage of aerosol particles through fibrous filters. *Dokl. Akad. Nauk SSSR* 195 (1-3): 71-74 (in Russian). English translation, *Sov. Phys. Dokl.* 15 (11): 1047-1049.
- Gunn, C.A., and J.B. McDonough. 1980. Survey of loading performance of currently available types of HEPA filters under in-service conditions. *Proc. 16th DOE Nuclear Air Cleaning Conf.* (CONF-801038, NTIS)
- Hollingsworth, M., Jr. 1978. A new filter media resistance tester. *ASHRAE Transactions* 84 (1): 590-599. Atlanta: American Society of Heating, Refrigerating and Air-Conditioning Engineers, Inc.
- Iinoya, K.K., K. Makino, and T. Imamura. 1970. Dust collection performance of paper filters. *Kagaku Kogaku* 34 (6): 632-637 (Eng. abstr.).
- Jonas, L.A., C.M. Lochboehler, and W.S. Magee, Jr. 1972. Aerosol filtration by fibrous filter mats. *Envir. Sci. & Tech.* 6 (9): 821-826.

- Kirsch, A.A., I.B. Stechkina, and N.A. Fuchs. 1973. Effect of gas slip on the pressure drop in fibrous filters. *J. Aerosol Sci.* 4: 287-293.
- Machine Design. 1985. Materials reference issue: Section 3, plastics, 57 (8): 143-206.
- Magee, W.S., Jr., L.A. Jonas, and W.L. Anderson. 1973. Aerosol filtration by fibrous filter mats. *Envir. Sci. & Tech.* 7 (13): 1131-1135.
- Monson, D.R. 1986. Key parameters used in modeling pressure loss of fibrous filter media. *Fluid Filtration: Gas*, ASTM STP 975 (1): 27-45. Philadelphia: ASTM.
- Murphy, D.J., Jr., and R.D. Rivers. 1997. *Determination of air filter performance under variable air volume conditions—Parts I and II*. Atlanta: American Society of Heating, Refrigerating and Air-Conditioning Engineers, Inc.
- Natanson, G.L. 1962. Influence of slip on impaction efficiency for capture of aerosols by a cylinder. *Kolloid. Zhurn.* 24 (1): 52-54 (in Russ.).
- Ogorodnikov, B.I., V.I. Skitovich, and V.I. Khabarov. 1976. Pressure distribution in gas flow in the presences of a fibrous filter in the channel. *J. Eng. Phys.* 31 (2): 922-924 (in Russ.).
- Pich, J. 1966. Theory of fibrous filters. *Aerosol Science*, pp. 223-286. London: Academic Press.
- Pui, D.Y.H., D.R. Chen, and B.Y.H. Liu. 1991. Optimization of pleated filter design using a finite-element numerical method. *J. Aerosol Sci.* 24 (Supp. 1): S39-S40.
- Raber, R.R. 1982. Pressure drop optimization and dust capacity estimation for a deep-pleated industrial air filter using small sample data. *Filtration & Separation* 19 (6): 508-511.
- Rivers, R.D. 1990. Air filtration and air pollution control equipment. *Handbook of HVAC Design*. New York: McGraw-Hill.
- Rüdinger, V., and J.G. Wilhelm. 1982. HEPA filter response to high air flow velocities. *Proc. 17th DOE Nuclear Air Cleaning Conf.*
- Schaefer, J.W., M.A. Barris, and B.Y.H. Liu. 1986. Filter media design for high purity applications. *J. of the Environmental Sciences* 29 (4): 27-31.
- Spielman, L., and S.L. Goren. 1968. Model for predicting pressure drop and filtration efficiency in fibrous media. *Envir. Sci. and Tech.* 2 (4): 279-287.
- Tosun, I., and M.S. Willis. 1983. Drag stress—Pressure drop relationships in filtration. *Chem. Eng. Sci.* 38 (3): 485-487.
- Ushakova, E.N., V.I. Kozlov, and I.N. Petrayanov. 1973. Hydrodynamics of FP filter materials. *Kolloid. Zhur.* 37 (1): 99-104 (Eng tr.).
- Weast, R.C., and M.J. Astle, eds. 1979. *CRC handbook of chemistry and physics*, 60th ed. Boca Raton: CRC Press.
- Wheat, J.A. 1963. Airflow resistance of glassfiber paper. *Canadian. J. Chem. Eng.* 41 (4): 67.
- Yeh, H.C., and B.Y.H. Liu. 1974. Aerosol filtration by fibrous filters—I. theoretical. *J. Aerosol Science* 5: 191-204.